Magnetoresistance and magnetization of Fe/Cr(001) superlattices with noncollinear magnetic ordering

V. V. Ustinov, N. G. Bebenin, L. N. Romashev, V. I. Minin, M. A. Milyaev, A. R. Del, and A. V. Semerikov
Institute of Metal Physics, Ural Division of the Russian Academy of Sciences, GSP-170, Ekaterinburg, 620219, Russia
(Received 6 May 1996; revised manuscript received 12 August 1996)

We study the magnetization and magnetoresistance of superlattices with biquadratic exchange. The equilibrium states are analyzed on the base of the free energy expression that includes all terms up to the fourth order in components of magnetizations of magnetic sublattices. The correlation between the magnetization curve and the magnetoresistance for various orientation of magnetic field relative to the film plane is established. The experimental studies are made on the samples of molecular-beam epitaxy grown Fe/Cr superlattices. The *positive* magnetoresistance was found for the perpendicular-to-plane magnetic field. It is shown that this effect as well as the characteristic features of the magnetization curves are connected with the noncollinear magnetic alignment, which exists in our samples, and the fourth order magnetic anisotropy of unfamiliar type. [S0163-1829(96)08745-0]

I. INTRODUCTION

Since the discovery of the giant magnetoresistance effect in the Fe/Cr superlattices,[1] the artificially made materials consisting of alternating layers of magnetic and nonmagnetic metals attract a great attention. The stimulus is perspectives of applications.[2] The main efforts are made to understand how magnetoresistance (MR) depends on the thickness of the magnetic layers as well as the nonmagnetic spacer, temperature, and magnetic field strength. The effect of orientation of magnetic field on MR remains less studied although it has been established already in Ref. 1 that this dependence is essential; the results of the FMR experiments on Co/Ru/Co trilayers[3] also confirm that the measurements at the various field orientation can be very instructive.

MR reflects the magnetic state of a multilayer—generally in a very complicated manner. It is believed, however, that the magnetoresistance r is mainly a function of the angle between the magnetization of neighboring magnetic layers only, i.e., of the absolute value of the relative (with respect to the saturation value) magnetization $\mathbf{m}$ of the superlattice: $r = \varphi(m)$. As long as it is true, the problem of understanding the orientation dependence of MR is reduced to two separated problems: the determination of $\varphi(m)$ and the determination of m in a given magnetic field.

The first problem is far from being solved; fortunately, in some cases it is sufficient to know only the basic properties of $\varphi(m)$, which are more or less simple, rather than its explicit form. As for the second, the magnetic alignment in a superlattice may be very specific. The point is that the exchange coupling between magnetic layers is governed by the spacer thickness, so that one can create multilayers with various magnetic ordering. It was found that this coupling oscillates with interlayer thickness between ferromagnetic (FM) and antiferromagnetic (AF). The system Fe/Cr(001) was found to exhibit AF exchange coupling.[4] Oscillation behavior of exchange interaction was discovered in Fe/Cr and other multilayers.[5] The evidence of FM and AF ordering in Fe/Cr was demonstrated in SEMPA studies of trilayers with a wedge shaped Cr interlayer.[6]

It is to be noted that FM and AFM alignments do not exhaust all possible magnetic structures in multilayers. The noncollinear 90° coupled magnetic profile in Fe/Cr trilayer was reported in Ref. 7. The coupling angle of 50° between the magnetizations of neighboring Fe layers have been discovered in Fe/Cr superlattices by spin polarized neutron reflectometry.[8] The noncollinear magnetic ordering in the MBE grown Fe/Cr superlattices has also been found and studied by magneto-optical methods.[9] It has also been demonstrated in Ref. 9 that the angle Θ_0 between the magnetizations of neighboring Fe layers in zero magnetic field varies with Cr interlayer thickness.

Phenomenological description of a magnetic alignment deviated from a collinear one is performed usually in terms of biquadratic exchange. In contrast to a bulk crystal, in a multilayer the usual bilinear exchange can be made very weak and hence the biquadratic exchange, reported in Ref. 7 for the trilayer, may play an important role. The microscopic origin of noncollinear ordering remains unclear, perhaps, it is different in different samples. Thus according to Slonczewski,[10] the biquadratic exchange can result from the interlayer thickness variation in the sample plane that leads to the fluctuation of the usual bilinear exchange near zero level. As a consequence, the intermediate coupling angle between the magnetizations of neighboring magnetic layers results. There are also other theoretical models which predict appearance of biquadratic coupling due to peculiarities of the interlayer magnetic[11] or electronic[12–17] structure; the last mechanisms are, however, too weak to explain the strong biquadratic coupling observed in Fe/Cr superlattices. In the present paper we will not discuss the nature of biquadratic exchange; a brief review of the theoretical results has been made recently by Slonczewski.[18]

The existence of relatively strong biquadratic exchange indicates that in multilayers the terms of the fourth order in the free energy expansion in components of the layers magnetizations may be essential although in a bulk crystal these terms are, as a rule, of no interest. Hence one may think that unfamiliar magnetic interactions as well as magnetic states of unusual type can be found in multilayers.

The aim of the present article is to show that in our MBE

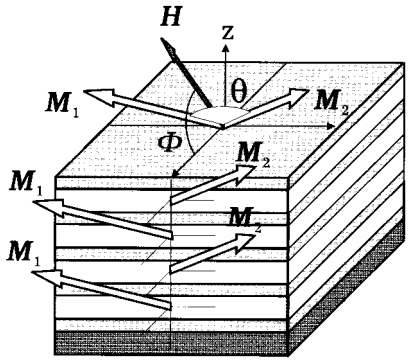

FIG. 1. Scheme of magnetic superlattice.

grown Fe/Cr superlattice samples with noncollinear magnetic ordering, the anisotropic interaction of the fourth order, which has never been observed and analyzed, really exists and that this interaction results in *positive* MR in magnetic field directed perpendicular to the layers plane. The article is organized as follows. In Sec. II the theoretical model is formulated and the free energy expression is written down in explicit form. In Sec. III the equilibrium states in zero- and non-zero-magnetic field are analyzed for the cases of the in-plane and the perpendicular-to-plane magnetization. In Sec. IV we describe the main properties of $\varphi(m)$ and show how MR can depend on the field strength at the various field orientation. Section V is devoted to some experimental details. The results of measurements and their interpretation are given in Sec. VI. Section VII is the Conclusions.

II. FREE ENERGY

Let us consider the superlattice consisting of the magnetic layers of thickness d_m, separated by the layers of nonmagnetic metal; see Fig. 1. We assume that our superlattice can be treated as a sum of two magnetic sublattices. The magnetization of a layer belonging to the first sublattice is $\mathbf{M}_1$, the magnetization of a layer of the second one is $\mathbf{M}_2$, and $|\mathbf{M}_1|=|\mathbf{M}_2|=M_0$. The free energy (per unit area and per one magnetic cell) of the superlattice placed in a constant magnetic field $\mathbf{H}$ directed under the angle Φ with respect to the layers plane can be written as

$$\begin{aligned} F=&-J_1\frac{\mathbf{M}_1\mathbf{M}_2}{M_0^2}-J_2\frac{(\mathbf{M}_1\mathbf{M}_2)^2}{M_0^4}-K_1\frac{(M_{1z}^2+M_{2z}^2)}{M_0^2}\\ &-K_2\frac{(M_{1z}^4+M_{2z}^4)}{M_0^4}+L_1\frac{M_{1z}M_{2z}}{M_0^2}+L_2\frac{(M_{1z}M_{2z})^2}{M_0^4}\\ &+L_3\frac{(\mathbf{M}_1\mathbf{M}_2)(M_{1z}M_{2z})}{M_0^4}+L_4\frac{(\mathbf{M}_1\mathbf{M}_2)(M_{1z}^2+M_{2z}^2)}{M_0^4}\\ &+L_5\frac{(M_{1z}M_{2z})(M_{1z}^2+M_{2z}^2)}{M_0^4}+2\pi d_m(M_{1z}^2+M_{2z}^2)\\ &-d_m\mathbf{H}(\mathbf{M}_1+\mathbf{M}_2). \end{aligned} \tag{1}$$

We suppose that the z axis of coordinate system is perpendicular to interfaces and that magnetocrystalline anisotropy in (x,y) plane can be neglected. A study of magnetic behavior of multilayer systems of cubic and uniaxial in-plane anisotropy has been reported in Refs. 19 and 20 but in those articles the biquadratic exchange has not been taken into consideration. The expression (1) includes all terms up to the fourth order in components of $\mathbf{M}_1$ and $\mathbf{M}_2$. The first two terms in (1) are bilinear and biquadratic exchange, respectively, the third and the fourth appear because of the anisotropy within magnetic layers, the next five are due to the anisotropic interaction between magnetic layers through a spacer, the last two describe the demagnetization and the interaction with external magnetic field.

We shall not find out the microscopic mechanism that leads to (1) and shall treat J's, K's, and L's as a phenomenological quantities that depend on the layers materials, values of thickness, etc.

The expression for F can be simplified by introducing the new variables $\mathbf{m}$ and $\mathbf{l}$ defined by

$$\mathbf{m}=\frac{\mathbf{M}_1+\mathbf{M}_2}{2M_0},\quad \mathbf{l}=\frac{\mathbf{M}_1-\mathbf{M}_2}{2M_0},$$

$$m^2+l^2=1,\quad (\mathbf{ml})=0. \tag{2}$$

It follows from (1) and (2)

$$\begin{aligned} F=&\frac{A_1}{2}m^2+\frac{A_2}{4}m^4+\frac{B_1}{2}m_z^2+\frac{B_2}{4}m_z^4+\frac{C_1}{2}m^2m_z^2\\ &+\frac{C_2}{2}m^2l_z^2+\frac{D}{2}m_z^2l_z^2+\frac{F_1}{2}l_z^2+\frac{F_2}{4}l_z^4-\mathbf{hm}. \end{aligned} \tag{3}$$

Here $\mathbf{h}=2d_mM_0\mathbf{H}$; A's, B's, etc., are linear combinations of J's, K's, and L's, for example, $A_1=-4J_1+8J_2$ and $A_2=-16J_2$. The complete set of the relations between coefficients in (1) and those in (3) are given in Appendix A. We have omitted in (3) the constant J_1-J_2 which is of no interest.

The right-hand side of (3) contains the anisotropy terms

$$\frac{C_1}{2}m^2m_z^2+\frac{C_2}{2}m^2l_z^2, \tag{4}$$

which are rather unfamiliar. As there are both isotropic (m^2) and anisotropic (m_z^2 or l_z^2) multipliers, one may call this anisotropy the fourth-order-exchange-uniaxial anisotropy.

Of course, (2) is applicable to any uniaxial antiferromagnet. However, in usually investigated antiferromagnetic crystals, m and m_z are very small. In a superlattice the biquadratic exchange interaction between layers can be relatively strong, so the effects related to the exchange-uniaxial anisotropy may be observed.

III. STABLE STATES

To describe the magnetization process, one has to find minimum(s) of the free energy. The general analysis is too involved, and hence it is desirable to simplify the problem. Notice that the demagnetization field acting upon the magnetic moments makes them to lie, as a rule, in the film plane if the external field is absent. So we shall restrict ourselves by considering an easy plane sample and set $l_z=0$ everywhere. The results of experiments described in Sec. VI show that this constraint is valid for our samples. Of course, there may exist the multilayers with biquadratic exchange and

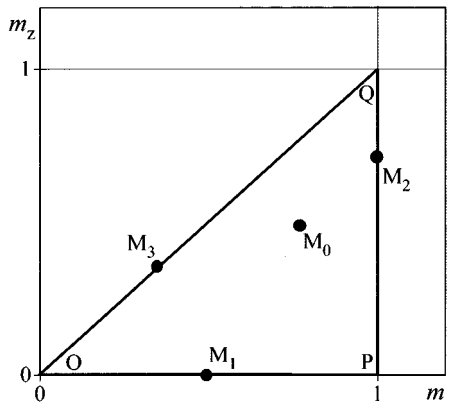

FIG. 2. Domain of definition of $F(m,m_z)$ and possible points of the free energy minimum in zero magnetic field.

with $l_z \neq 0$. Such a situation has been demonstrated to occur if the uniaxial anisotropy renders the z direction an easy direction,[21] and we are referring a reader to that article to find the detailed analysis.

In what follows we shall for brevity write $F(m,m_z,h)$ instead of the more correct $F(m,m_z,l_z=0,h)$.

The domain of definition of $F(m,m_z,h)$ on (m,m_z) plane is ΔOPQ with vertices $O=O(0,0)$, $P=P(0,1)$, and $Q=Q(1,1)$. The free energy reaches a minimum either at an internal point of the triangle or/and at a vertex, or/and at an internal point of a side of ΔOPQ; see Fig. 2. For the sake of simplicity we assume that all the points mentioned are different.

A. H=0

If $\mathbf{h}=0$, it is convenient to consider the free energy $F(m,m_z,h=0)\equiv F_0(m,m_z)$ as a function of $\zeta=m^2$ and $\eta=m_z^2$ rather than m and m_z. From (3) it follows

$$F(m,m_z)=\Psi(\zeta,\eta)=\frac{A_1}{2}\,\zeta+\frac{A_2}{4}\,\zeta^2+\frac{B_1}{2}\,\eta+\frac{B_2}{4}\,\eta^2+\frac{C_1}{2}\,\zeta\eta. \tag{5}$$

The domain of definition of Ψ on (ζ,η) plane is $\Delta O'P'Q'$ with $O'=O'(0,0)$, $P'=P'(0,1)$, and $Q'=Q'(1,1)$. Our aim is to determine the location of minimum(s) of Ψ.

Let us define the surface S over the (ζ,η) plane by the relation $\xi=\Psi(\zeta,\eta)$. It is a second degree surface. If $\Delta=A_2B_2-C_1^2>0$, S is an elliptic paraboloid; if $\Delta<0$, S is a hyperbolic paraboloid. Partial derivatives $\partial\Psi/\partial\zeta$ and $\partial\Psi/\partial\eta$ are equal to zero at $M_0'(\zeta_0,\eta_0)$ with coordinates

$$\zeta_0=\frac{B_1C_1-A_1B_2}{\Delta},\quad \eta_0=\frac{A_1C_1-A_2B_2}{\Delta}. \tag{6}$$

M_0' corresponds to the bottom of S if $A_2>0$, $\Delta>0$, the top of S if $A_2<0$, $\Delta>0$, and a saddle point if $\Delta<0$. If M_0' corresponds to the bottom of S and M_0' belongs to $\Delta O'P'Q'$, the minimum of Ψ is at this point: otherwise a minimum lies at the boundary of the domain, i.e., at an internal point of a side and/or at a vertex of $\Delta O'P'Q'$. The conditions, which are sufficient for a minimum of Ψ to be at one of the points mentioned, are given in Appendix B.

One can easily verify that if $A_2>0$, $\Delta>0$, the minimum is unique whether M_0' belongs to the triangle or not. If A_2 or Δ is negative, the number of minimum is one, two, or three but not more, because if Ψ reaches its minimum at a vertex, there is no minimum at an adjacent side of the triangle.

B. H≠0

For simplicity we shall assume that a magnetic field is applied either along the film plane or perpendicular to the plane, so that $\mathbf{hm}=hm$ or $\mathbf{hm}=hm_z$; then $F(m,m_z,h)$ turns out to be a polynomial. Unfortunately even in these cases a general analysis involves many parameters and is too cumbersome to be instructive. In this situation we restrict ourselves (without much originality) by considering some particular cases.

Let us suppose that a minimum of $F(m,m_2,\mathbf{h}=0)$ can lie only on OP side of ΔOPQ. This means that both $\mathbf{M}_1$ and $\mathbf{M}_2$ lie in the xy plane. At first we consider the in-plane magnetization. Equating m_z to zero, we obtain from (3)

$$F=\frac{A_1}{2}\,m^2+\frac{A_2}{4}\,m^4-hm. \tag{7}$$

A simple examination of (7) leads to the following conclusions.

(1) When $A_1>0$, $2A_1+A_2>0$ (or, in other notations, $J_1<0$, $J_1-2J_2<0$), the equilibrium state at $H=0$ is antiferromagnetic one. Corresponding region is shown in Fig. 3 as a sum of three regions: AFM1, AFM2, and AFM3.

AFM1 region. If $A_1>0$, $A_1+3A_2>0$ (i.e., $J_1-2J_2<0$, $J_1+10J_2<0$), the equilibrium state at $H=0$ is antiferromagnetic one. If $h<h_1$, the relative magnetization m obeys the relation

$$h=A_1m+A_2m^3, \tag{8}$$

where $h_1=A_1+A_2$; if h exceeds h_1, then $m=1$. The magnetization curve, sketched in Fig. 4, is convex downward, if A_2 is positive, and upward if it is negative.

AFM2 region. When $A_1+3A_2<0$, $A_1+A_2>0$ (i.e., $J_1+10J_2>0$, $J_1+2J_2<0$), the local minimum appears at $m=1$ if h exceeds h_1. The state with $m\neq 1$ remains, however, stable if $h<h_2$ with

$$h_2=\tfrac{2}{3}\,A_1\sqrt{A_1/3|A_2|}. \tag{9}$$

Thus the first order phase transition takes place at the field lying between h_1 and h_2, the width $\delta h=h_2-h_1$ of the hysteresis loop being determined by the *isotropic* interaction.

AFM3 region. When inequalities $A_1>0$, $A_1+A_2<0$ ($J_1-2J_2<0$, $J_1+2J_1>0$) are satisfied, there are two minimums in zero magnetic field: one is at $m=0$ and the second is at $m=1$. If $A_1+A_2<0$, $2A_1+A_2>0$, ($J_1+2J_2>0$, $J_1<0$), then at $h=0$ the antiferromagnetic state is realized because it has a lower energy than ferromagnetic one. If in this case h is increased from zero to a value which is less than h_2 and after that the field is decreased back to zero, the system returns into the initial antiferromagnetic state. But if h reaches h_2, the system jumps into the ferromagnetic state. Once there, the superlattice cannot leave this state even

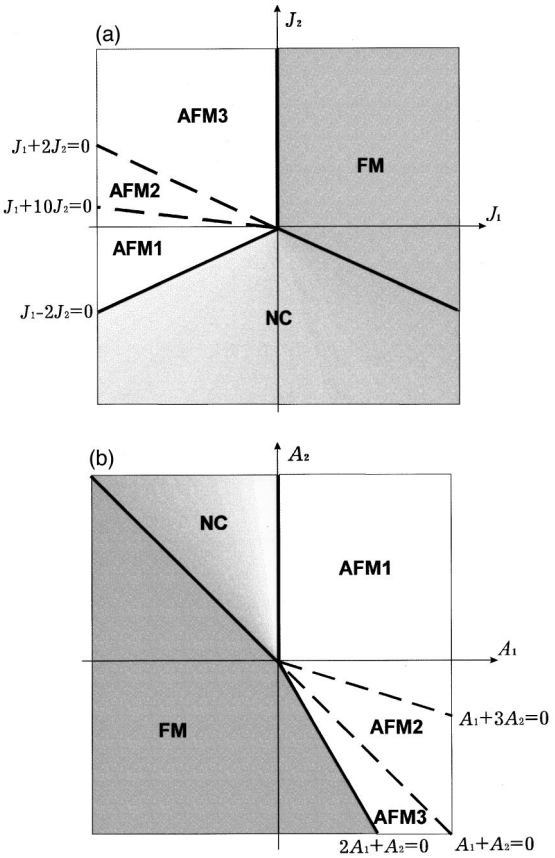

FIG. 3. Phase diagram on (J_1,J_2) and (A_1,A_2) planes, (a) and (b), respectively.

after the field is switched off because this state is stable at arbitrary field strength. As a consequence after the jump the multilayer looks like an ordinary ferromagnet whatever the field strength although the true equilibrium state is an antiferromagnetic one.

In the event $A_1>0$, $2A_1+A_2<0$. ($J_1>0$, $J_1-2J_2<0$) the ferromagnetic state always has a lower energy.

When inequalities $A_1<0$, $A_1+A_2>0$ are satisfied, i.e., $J_2<-|J_1|/2$, the noncollinear (canted) state with magnetization

$$m_0=\sqrt{|A_1|/A_2}=\sqrt{(J_1-2J_2)/4|J_2|} \tag{10}$$

exists at $h=0$, the angle Θ_0 between $\mathbf{M}_1$ and $\mathbf{M}_2$ being equal to $2a\cos m_0$. The magnetization versus magnetic field is again given by Eq. (8) until $h>h_1$.

The magnetic susceptibility for $h\to 0$ is given by

$$\chi_0\equiv\left.\frac{\partial m}{\partial h}\right|_{h=0}=\frac{1}{2|A_1|}. \tag{11}$$

At last, if both A_1 and A_2 are negative ($J_1-2J_2>0$, $J_2<0$), the system is in the ferromagnetic state.

Let us proceed to consider the perpendicular-to-plane magnetization. We shall discuss only one case which is the most interesting to us; namely, we shall assume that the noncollinear state is realized at $h=0$ and that there is no metastable state. It implies that inequalities $A_1<0$, $A_1+A_2>0$, $A_2B_1-C_1A_1>0$ are satisfied (see Appendix B). The equilibrium conditions are given by

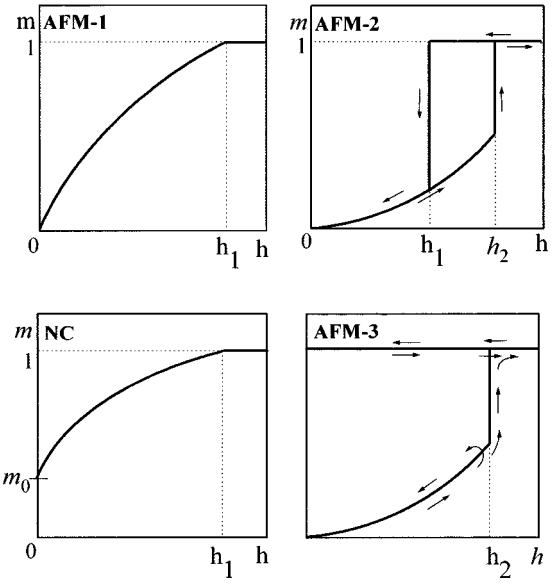

FIG. 4. Typical magnetization curves in the case of the in-plane magnetic field.

$$m(A_1+A_2m^2+C_1m_z^2)=0, \tag{12}$$

$$B_1m_z+B_2m_z^3+C_1m^2m_z-H=0. \tag{13}$$

It is assumed here that $m\neq m_z$, $m\neq 1$. Since $m\neq 0$, it follows from (12)

$$m^2=m_0^2-\frac{C_1}{A_2}m_z^2. \tag{14}$$

Substituting this into (13), we obtain

$$h=\frac{A_2B_1-A_1C_1}{A_2}m_z+\frac{\Delta}{A_2}m_z^3. \tag{15}$$

The linear term in the right-hand side of (15) is positive while the sign of the second term coincides with the sign of Δ.

These formulas show that the equilibrium point moves on (m,m_z) plane as magnetic field is increased. A trajectory consists of two parts; see Fig. 5. The first one begins at M_1 on OP and ends at $h=h_c$ at the second order phase transition point M_c which lies on OQ or PQ; this part of the trajectory is described by the relations (12)–(15). Farther the point of equilibrium moves along the corresponding side of the triangle towards the vertex Q where the movement terminates.

If $C_1=0$, the first part of the trajectory is the vertical straight line. It means that the magnetization vectors of the sublattices go out of the film plane with increasing magnetic field in such a way that the angle Θ between these vectors remains fixed until the plane to which the vectors belong becomes perpendicular to the film plane; further Θ decreases till zero. When the equilibrium point moves along OQ, the magnetization $m=m_z$ obeys the equation

$$h=(A_1+B_1)m_z+(A_2+B_2)m_z^3, \tag{16}$$

which is valid until $m=m_z=1$.

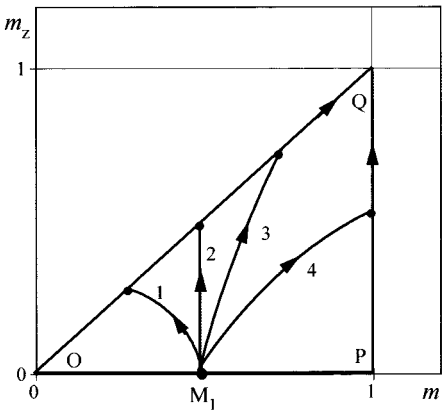

FIG. 5. The trajectories of the equilibrium point on (m,m_z) plane in the case of the perpendicular-to-plane magnetic field: (1) $C_1>0$; (2) $C_1=0$; (3) $C_1<0$, $|C_1|<A_2(1-m_0^2)$; (4) $C_1<0$, $|C_1|>A_2(1-m_0^2)$.

If $C_1>0$, the trajectory of the point of equilibrium deviates from the vertical straight line to the left. The critical value $m_c=m(h_c)$ of the magnetization can be found from (14). One gets

$$m_c=\frac{m_z}{\sqrt{1+C_1/A_2}}. \tag{17}$$

If h exceeds h_c, which is found from (15) by setting $m_z=m_c$, the magnetization curve is described by the relation

$$h=(A_1+B_1)m_z+(A_2+B_2+2C_1)m_z^3. \tag{18}$$

Notice that in the case $C_1>0$ the angle between the magnetization vectors first increases and only if $h>h_c$ this angle decreases with increasing field.

If $C_1<0$, the point of equilibrium deviates from the vertical straight line to the right and reaches OQ or PQ depending on whether $|C_1|$ is less or more than $A_2(1-m_0^2)$. In the later case Θ vanishes at M_c, so that at $h>h_c$ the magnetization vector of the superlattice turns to the symmetry axis just like in an ordinary ferromagnet. If $|C_1|<A_2(1-m_0{}^2)$, the equation (18) is valid; otherwise

$$h=(B_1+C_1)m_z+B_2m_z^3 \tag{19}$$

until the magnetization is parallel to the z axis.

The examples considered above show that the magnetization curves of a multilayer with sufficiently large terms of the fourth order may be rather unusual. The interesting point is that there can be the metastable states because the existence of these states can lead to an incorrect conclusion about the equilibrium magnetic ordering. But even if these states are absent, one can hit upon such unfamiliar fact as the decrease of absolute value of the magnetization vector of the superlattice with increasing magnetic field.

IV. MAGNETORESISTANCE

When magnetic field is applied, the resistance of a sample changes. The magnetoresistance r is defined by

$$r=\frac{R_H-R_0}{R_0}, \tag{20}$$

where R_H denotes the resistance in the presence of magnetic field, $R_0=R_{H=0}$. Generally, the magnetoresistance depends on the direction of the electric current as well as that of the magnetization of the multilayer. In the most experiments, including those described in the next section, the current flows in the film plane. In this case, r is nearly unaffected by varying the orientation of the current. It is not our aim here to discuss this anisotropy and, as is stated in the Introduction, we ignore it assuming that r is a function of m only: $r=\varphi(m)$, where $m=m(H,\Phi)$.

Both theory and experiments say that $\varphi(m)$ is a monotone decreasing function. The features of magnetic state of a multilayer are then clearly reflected in **H** dependence of magnetoresistance. For example, if at $H=0$ the noncollinear magnetic ordering exists, in the case $\Phi=0$ the magnetoresistance is a monotone decreasing function of H until saturation because m monotonically increases.

On the contrary, in the case of the perpendicular-to-plane magnetization the magnetoresistance may be a monotone decreasing function of H (until saturation), or be a nonincreasing one, or even have a maximum at the second order phase transition point when $h=h_c$, as it follows from the theoretical results described above. Another interesting point is the following. The saturation of the magnetoresistance and that of the magnetization of a multilayer may take place either in one and the same magnetic field or the magnetoresistance is saturated in a lower field than magnetization; the last case occurs if $C_1<0$ and $|C_1|>A_2(1-m_0{}^2)$.

If the measurements of the magnetoresistance are performed at the angles which are not necessarily equal to 0° or 90°, the functions $r(H,\Phi)$ for various Φ's may not be completely independent. The question is how to calculate r for arbitrary Φ if the magnetoresistance for some certain Φ's is known. The answer can be formulated as follows. Let us fix the value r of magnetoresistance. Then the relation

$$\varphi(m(H,\Phi))=r \tag{21}$$

defines the implicit function $H_r(\Phi)$. It follows that

$$\frac{\partial m}{\partial H}\frac{\partial H_r(\Phi)}{\partial \Phi}+\frac{\partial m}{\partial \Phi}=0. \tag{22}$$

Finding $\partial m/\partial\Phi$ and $\partial m/\partial H$ by making use of the expression for the free energy, one can obtain a differential equation for $H_r(\Phi)$ and hence find this function. This program has been realized in Ref. 22 for the case when the anisotropy terms of the fourth order are absent. The equation for $H_r(\Phi)$ has the form

$$\frac{\partial}{\partial\Phi}\left(\frac{1}{\sin(2\Phi)}\frac{\partial}{\partial\Phi}\frac{1}{H_r^2(\Phi)}\right)=0. \tag{23}$$

The result of solving (23) can be written as

$$H_r(\Phi)=\left(\frac{\cos^2\Phi}{H_r^2(0°)}+\frac{\sin^2\Phi}{H_r^2(90°)}\right)^{(1/2)}. \tag{24}$$

The solution $H_r(\Phi)$ contains two arbitrary constants which are nothing but the values of this function $H_r(0°)$ and

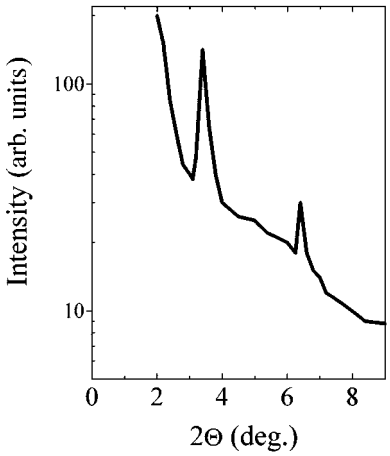

FIG. 6. Low-angle x-ray diffraction pattern of the $[Fe(23\ Å)/Cr(8\ Å)]_{30}$ sample.

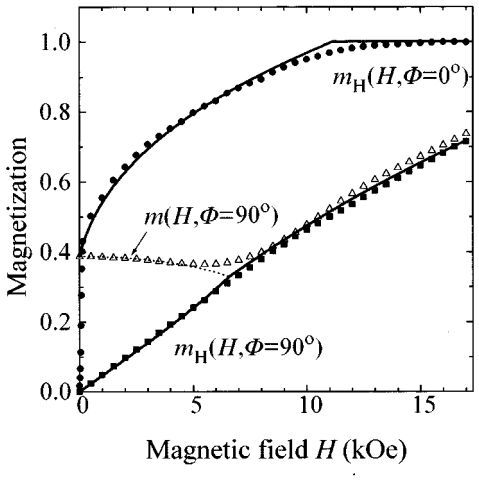

FIG. 7. Magnetization curves of the $[Fe(23\ Å)/Cr(8\ Å)]_{30}$ sample for the in-plane and the perpendicular-to-plane magnetic field.

$H_r(90°)$ at the boundary of the domain of definition. It is to be noted that (24) does not contain any parameters that characterize the interaction between adjacent layers.

Obviously, m must be a continuously differentiable function and $\partial m/\partial H$ must be nonzero everywhere in order for this method to be valid. For example it is inapplicable for those values of the field strength for which the magnetoresistance has an extremum.

V. EXPERIMENT

The $(Fe/Cr)_{30}$ samples were grown by the molecular-beam epitaxy method on MgO(100) substrate. The chromium buffer was about 100 Å. In different samples the Fe layers varied from 10 to 30 Å in thickness; the Cr spacer was from 10 to 30 Å in thickness. Every sample was covered with a protective Cr layer.

The vibrating sample magnetometer (VSM) was used in measuring magnetization. The magnetometer allows us to determine the projection m_H of the magnetization **m** onto magnetic field direction. The resistance was measured by the standard four-probe method. The temperature was 290 and 77 K.

The low-angle x-ray diffraction pattern of a typical sample presented in Fig. 6 clearly indicates that our multilayers have a layered structure of satisfactory quality.

VI. RESULTS AND INTERPRETATION

We present here the results concerning the properties of only one sample $[Fe(23\ Å)/Cr(8\ Å)]_{30}$ at room temperature which demonstrates all the features we would like to discuss. The detailed analysis of the dependence of the physical properties on the layers thickness and temperature will be published elsewhere.

Shown in Fig. 7 is the magnetic field dependence of $m_{\mathbf{H}}$. If **H** lies in the film plane, the magnetization curve $m_{\mathbf{H}}(H,\Phi=0°)=m(H)$ (solid circles) is smooth and convex upward. It is to be noted that in a weak field, $H<150$ Oe, the magnetization is determined by the domain walls displacement and by the in-plane anisotropy, therefore this region is excluded from our consideration. The value of magnetization $m(H)$ near $H=0$ but outside the region of domain walls displacement is equal to $m_0=0.39$. If **H** is perpendicular to the plane, i.e., $\Phi=90°$, the magnetization curve $m_{\mathbf{H}}(H,\Phi=90°)=m_z(H)$ (solid squares) has a weak peculiarity near 6 kOe one can easily confirm the existence of the peculiarity by plotting $\partial m_r/\partial H$ vs H curve. No jumps on a magnetization curve were observed. The magnetization curves at 77 and 290 K are practically identical.

Figure 8 shows the magnetic field strength dependence of magnetoresistance for the in-plane $(r_\parallel)$ and the perpendicular-to-plane $(r_\perp)$ magnetization. In the first case the resistance does not depend on the angle between **H** and the current and we restrict ourselves by presenting the data referred to the case $\mathbf{H}\|\mathbf{j}$. As magnetic field grows up, the longitudinal magnetoresistance $r_\parallel$ is negative and decreases until saturation. The perpendicular magnetoresistance $r_\perp$ is positive if $H<8$ kOe and has a maximum at $H=6$ kOe. The saturation value of $r_\perp$ is equal to that of $r_\parallel$. The saturation fields found from the VSM data and from the MR are equal to each other.

Using the data for $r_\parallel$ and the VSM data for $m_{\mathbf{H}}(H,\Phi=0°)$ we have determined $\varphi(m)$. The result is pre-

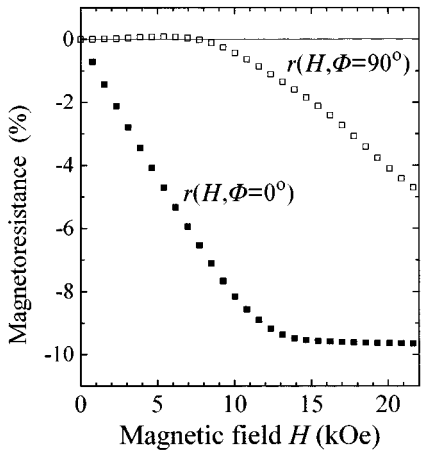

FIG. 8. The longitudinal ($\Phi=0°$) and perpendicular ($\Phi=90°$) magnetoresistance.

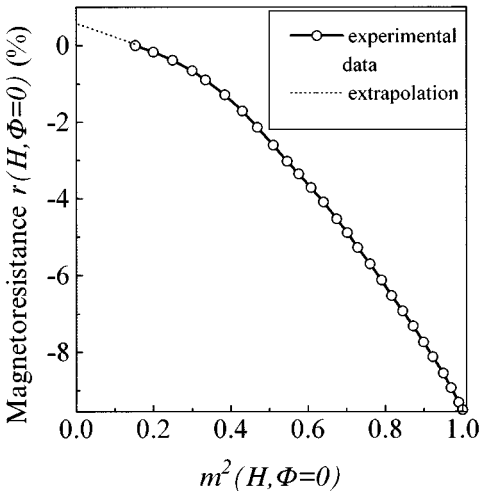

FIG. 9. Longitudinal MR vs m^2. Dots are extrapolation to small ($m<m_0$) values of m.

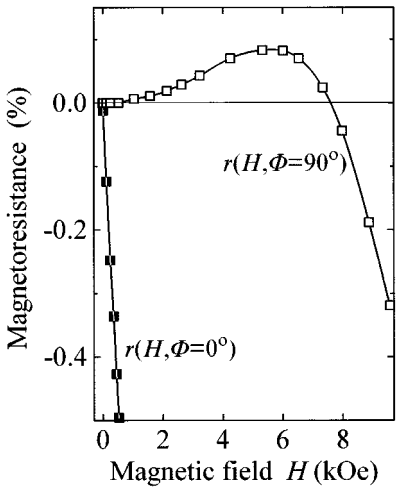

FIG. 10. $r(H,\ \Phi=90°)$ and $r(H,\ \Phi=0°)$ at low magnetic field.

sented in Fig. 9 by circles. It is evident that $\varphi(m)$ deviates from the simplest one $\varphi(m)\propto m^2$. The possible model for describing such a deviation has been developed in Refs. 23 and 24. It has been shown there that $\varphi(m)$ is proportional to m^2 only in the case of antiferromagnetic ordering in zero field for small values of m while for arbitrary m in the case of noncollinear ordering

$$r_{\parallel}=r_s\,\frac{\delta(m)-\delta(m_0)}{1-\delta(m_0)}, \tag{25}$$

where r_s is the saturation value of $r_{\parallel}$,

$$\delta(m)=\frac{\alpha m^2+\beta m^4}{1-(1-\alpha-\beta)m^2}. \tag{26}$$

The parameters α and β depend on the conduction electrons spin scattering inside the layers and at the interfaces. Solid curve in Fig. 9 is the approximation of experimentally obtained $\varphi(m)$ by expressions (25) and (26) with $\alpha=0.41$ and $\beta=0.42$. Formally, the function $\varphi(m)$ extracted from the data for $r_{\parallel}$ and the VSM data for $m_{\mathbf{H}}(H,\Phi=0°)$ is defined only for $m\geqslant m_0$. The approximation of $\varphi(m)$ by expression (25) gives us the possibility to calculate magnetoresistance for $m\leqslant m_0$. In fact we have used the quadratic extrapolation of $\varphi(m)$ to the region $m\leqslant m_0$ because $\mathbf{m}_0^2\approx 0.15$ is small. Knowing $\varphi(m)$ over the whole range $0\leqslant m\leqslant 1$ we are able to calculate the absolute value of magnetization $m(H,\Phi=90°)$ from the MR data for $r_{\perp}$ presented in Fig. 9. The result of this procedure is shown in Fig. 7 by triangles. We have obtained a rather unusual picture: at first $m(H,\Phi=90°)$ decreases with growing H. Minimum of $m(H,\Phi=90°)$ takes place at $H=6$ kOe.

So, we have the following experimental facts.

(1) The magnetization $m_{\mathbf{H}}(H,\Phi=0°)$ is nonzero in the nearest vicinity of $H=0$.

(2) The perpendicular resistivity $r_{\perp}$ does not change noticeably and is positive in a wide region of magnetic field up to 8 kOe.

(3) The resistivity $r_{\perp}$ grows in the range $0<H<6$ kOe despite the fact that $r_{\parallel}$ decreases monotonically and substantially in this range.

(4) Magnetization $m(H,\Phi=90°)$ decreases with growing H over the range $0<H<6$ kOe.

Comparing these facts with the theoretical results of Sec. IV we may conclude that a noncollinear magnetic ordering exists in the sample in zero magnetic field.

To confirm this statement, we have calculated the magnetization curve for the case of the in-plane **H** in accordance with (8). It is convenient to rewrite (8) as

$$H=\frac{H_s}{1-m_0^2}\,m(m^2-m_0^2), \tag{27}$$

where $H_s=(A_1+A_2)/2d_mM_0$ is the saturation field. The upper line in Fig. 7 is the result of calculations in accordance with (27). The saturation field has been taken to be 11 kOe, and $m_0=0.39$; these values correspond to $A_1/2d_mM_0=-2$ kOe and $A_2/2d_mM_0=13$ kOe or $J_1/2d_mM_0=-1.15$ kOe and $J_2/2d_mM_0=-0.82$ kOe. One can see that the calculated curve agrees well with the experimental points. The deviation exists only near H_s.

According to the consideration of Sec. IV, the decrease of $m(H,\Phi=90°)$ in the range $0<H<6$ kOe implies that C_1 is positive and that the critical field H_c is close to 6 kOe. Taking into account (14) and the fact that for $H<6$ kOe the magnetization m_z is approximately proportional to H, one may expect $r_{\perp}$ to be proportional to H^2 if $H<6$ kOe. It is easy to see from Fig. 10 that it is just the case.

We have calculated also the magnetization curves $m_{\mathbf{H}}(H,\Phi=90°)$ and $m(H,\Phi=90°)$ for the case of the perpendicular-to-plane **H** in accordance with (14), (15), and (18) with A_1 and A_2 as in the case of the in-plane **H**. The best fitting (see Fig. 7) corresponds to $H_c=6.6$ kOe, $B_1/2d_mM_0=21$ kOe, $B_2/2d_mM_0=-14$ kOe, and $C_1/2d_mM_0=5$ kOe. Now we easily find $m_c=0.33$ and obtain the estimation $C_1/A_2=0.38$. C_1 is small in comparison with A_2 and B_1; therefore the corresponding summand ($\propto C_1m^2m_z^2$) in the free energy expression (3) is insignificant if the equilibrium point is far enough from the critical one.

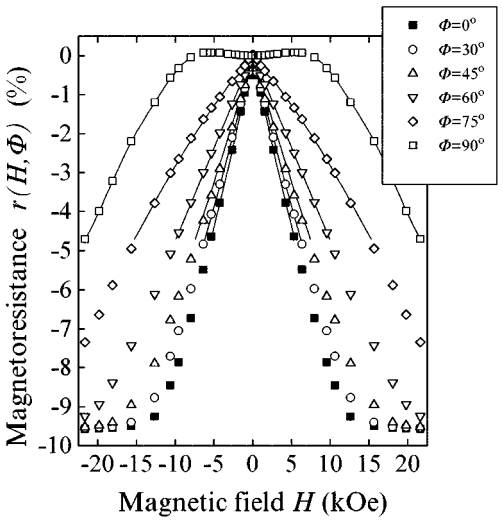

FIG. 11. Magnetoresistance of the $[Fe(23\ Å)/Cr(8\ Å)]_{30}$ sample at various orientation of magnetic field. The solid lines are the result of calculations in accordance with (24).

The term $\propto B_2 m_z^4$ is unessential as compared with the second order anisotropy term $\propto B_1 m_z^2$ at $m_z \ll 1$. Thus one may expect that the relation (24) hold in the range $0 < r \ll r_s$. Figure 11 shows r versus H measured for some Φ's; the solid lines are the results of calculations in accordance with (24). One can see that the theoretical curves are indeed in agreement with the experiment.

VII. CONCLUSIONS

(1) In our MBE grown Fe/Cr superlattice samples the biquadratic exchange interaction between magnetic layers results in the noncollinear magnetic ordering.

(2) New type of magnetic anisotropy in superlattices has been discovered. Taking into account all terms of the fourth order in the free energy expression, we have analyzed possible equilibrium states in zero magnetic field as well as the features of the magnetization curves for the in-plane and the perpendicular-to-plane magnetization. It has been found theoretically and observed in experiment that in the last case the specific second order phase transition takes place in a multilayer with the noncollinear ordering. In our samples the fourth order exchange-uniaxial anisotropy results in decreasing the absolute value of magnetization with increasing magnetic field.

(3) At low magnetic field the in-plane magnetoresistance of the superlattice with noncollinear structure is proportional to the field strength H whereas the perpendicular-to-plane magnetoresistance varies as H^2.

(4) The exchange-uniaxial anisotropy in our MBE grown Fe/Cr gives rise to the *positive* magnetoresistance in the perpendicular-to-plane magnetic field, the maximum of magnetoresistance taking place at the second order phase transition point.

ACKNOWLEDGMENTS

The authors are grateful to Professor H. Zabel for discussion on the noncollinear magnetic ordering and providing the manuscript of papers[8] prior to publication. The research described in this publication was made possible by Grant No. 95-02-04813 from the Russian Foundation of Basic Researches and Grant-in-Aid No. 1-053/2 for Research Program from the Ministry of Science of Russia.

APPENDIX A

The relations between coefficients that appear in Eq. (1) and in Eq. (3) are given by the following formulas:

$$A_1 = -4J_1 + 8J_2, \tag{A1}$$

$$A_2 = -16J_2, \tag{A2}$$

$$B_1 = -4K_1 + 2L_1 - 2L_3 - 4L_4 + 8\pi d_m M_0^2, \tag{A3}$$

$$B_2 = -8K_2 + 4L_2 + 8L_5, \tag{A4}$$

$$C_1 = 4L_3 + 8L_4, \tag{A5}$$

$$C_2 = -4L_3 + 8L_4, \tag{A6}$$

$$D = -24K_2 - 4L_2, \tag{A7}$$

$$F_1 = -4K_1 - 2L_1 + 2L_3 - 4L_4 + 8\pi d_m M_0^2, \tag{A8}$$

$$F_2 = -8K_2 + 4L_2 - 8L_5. \tag{A9}$$

APPENDIX B

Here we present the sufficient conditions for a minimum of Ψ to exist at a point mentioned. The local minimum is at $M_1'(\zeta_1,0)$ with $0<\zeta_1<1$ when

$$A_1<0, \quad A_2>0, \quad A_1+A_2>0, \quad A_2B_1 - C_1A_1>0. \tag{B1}$$

$M_2'(1,\eta_2)$ with $0<\eta_2<0$ is the point of minimum in the case

$$B_2>0, \quad B_1+C_1<0, \quad B_1+B_2+C_1>0. \tag{B2}$$

Ψ reaches the minimum at M_3' provided that

$$A_1+B_1<0, \quad A_2+B_2+2C_1>0, \tag{B3}$$

$$A_1+B_1+A_2+B_2+2C_1>0, \quad C_1-A_2B_1>B_1C_1-A_1B_2. \tag{B4}$$

The conditions in order for a minimum of Ψ to be at a vertex of the triangle can be formulated as follows. A minimum is at $A'(0,0)$ if

$$A_1>0, \quad A_1+B_2>0; \tag{B5}$$

at $B'(1,0)$ when

$$A_1+A_2<0, \quad B_1+C_1>0; \tag{B6}$$

at last a minimum is at $C'(1,1)$ in the case

$$B_1+B_2+C_1<0, \quad A_1+A_2+B_1+B_2+2C_1<0. \tag{B7}$$

The conditions in order for the minimum to be at M_0' are already given in Sec. III.

[1] M. N. Baibich, J. M. Broto, A. Fert, F. Nguyen van Dau, F. Petroff, P. E. Eitenne, G. Creuzet, A. Friedrich, and J. Chazelas, Phys. Rev. Lett. **61**, 2472 (1988).
[2] R. L. White, IEEE Trans. Magn. **30**, 346 (1994).
[3] Z. Zhang, L. Zhou, P. E. Wigan, and K. Ounadjela, Phys. Rev. B **50**, 6094 (1994).
[4] P. Grunberg, R. Schreiber, Y. Pang, M. D. Drodsky, and H. Sowers, Phys. Rev. Lett. **57**, 2442 (1986)
[5] S. S. P. Parkin, N. More, and K. P. Roche, Phys. Rev. Lett. **64**, 2304 (1990).
[6] R. d. Celotta, D. T. Pierce, and J. Unguris, MRS Bull. **20**, 30 (1995).
[7] M. Ruhrig, R. Schafer, A. Hubert, R. Mosler, J. A. Wolf, S. Democritov, and P. Grunberg, Phys. Status Solidi A **125**, 635 (1991).
[8] A. Schreyer, J. F. Ankner, M. Schäfer, Th. Zeidler, H. Zabel, C. F. Majkzak, and P. Grünberg, J. Magn. Magn. Mater. **148**, 189 (1995). A. Schreyer, J. F. Ankner, Th. Zeidler, M. Schäfer, H. Zabel, C. F. Majkzak, and P. Grünberg, Europhys, Lett. **32**, 595 (1995). A. Schreyer, J. F. Ankner, Th. Zeidler, H. Zabel, M. Schäfer, J. A. Wolf, P. Grünberg, and C. F. Majkzak, Phys. Rev. B **52**, 16 066 (1995).
[9] V. V. Ustinov, M. M. Kirillova, I. D. Lobov, V. M. Maevskii, A. A. Makhnev, V. I. Minin, L. N. Romashev, A. R. Del, A. V. Semerikov, and E. I. Shreder, J. Magn. Magn. Mater. **156**, 179 (1996); V. V. Ustinov, M. M. Kirillova, I. D. Lobov, V. M. Mayevskii, A. A. Makhnev, V. I. Minin. L. N. Romashev, A. R. Del, A. V. Semerikov, and E. I. Shreder, JETP **109**, 477 (1996).
[10] J. C. Slonczewski, Phys. Rev. Lett. **67**, 3172 (1991).
[11] J. C. Slonczewski, J. Appl. Phys. **73**, 5957 (1993).
[12] J. Barnas and P. Grunberg, J. Magn. Magn. Mater. **121**, 313 (1993).
[13] P. Bruno, J. Magn. Magn. Mater. **121**, 248 (1993).
[14] D. M. Edvards, J. M. Ward, and J. Mathon, J. Magn. Magn. Mater. **126**, 380 (1993).
[15] S. Demokritov, E. Tsymbal, P. Grunberg, W. Zinn, and I. Shuller, Phys. Rev. B **49**, 720 (1994).
[16] D. M. Edwards, A. M. Robinson, and J. Mathon, Phys. Met. Metallogr. **79**, 1 (1995).
[17] J. Mathon, Murielle Villeret, D. M. Edwards, and R. B. Muniz, Phys. Met. Metallogr. **79**, 5 (1995).
[18] J. Slonczewski, J. Magn. Magn. Mater. **150**, 13 (1995).
[19] B. Dieny, J. P. Gavigan, and J. P. Rebouillat, J. Phys. Condens. Matter **2**, 159 (1990).
[20] B. Dieny and J. P. Gavigan, J. Phys. Condens. Matter **2**, 187 (1990).
[21] N. S. Almeida and D. L. Mills, Phys. Rev. B **52**, 13 504 (1995).
[22] V. V. Ustinov, L. N. Romashev, V. I. Minin, A. V. Semerikov, and A. R. Del, Phys. Met. Metallogr. **80**, 71 (1995).
[23] V. V. Ustinov and E. A. Kravtsov, J. Phys. Condens. Matter **7**, 3471 (1995).
[24] V. V. Ustinov and E. A. Kravtsov, J. Magn. Magn. Mater. **148**, 307 (1995).